Polym. Bull. (2012) 69:389–403
DOI 10.1007/s00289-012-0729-7

ORIGINAL PAPER

Synthesis and characterization of hydrophobic long-chain fatty acylated cellulose and its self-assembled nanoparticles

Yanzhu Guo · Xiaohui Wang · Dong Li · Hong Du · Xiaoying Wang · Runcang Sun

Received: 3 October 2011 / Revised: 4 January 2012 / Accepted: 29 February 2012 /

Abstract In this paper, a series of cellulose-based hydrophobic associating polymers were prepared by homogeneous acylation of microcrystalline cellulose with long-chain acyl chlorides including octanoyl, lauroyl, and palmitoly chlorides in the solvent of *N,N*-dimethylacetamide/lithium chloride (DMAc/LiCl) using pyridine as acid scavenger. Through controlling the chain length of fatty acyl chlorides and the molar ratio of acyl chlorides vs anhydroglucose unit, the hydrophobic cellulose derivatives with degrees of substitution in the range of 0.02–1.75 were successfully obtained. The chemical structures and properties of these hydrophobic derivatives were characterized by elemental analysis, FT-IR, CP/MAS ^{13}C NMR, X-ray diffraction, and the thermogravimetry analysis. It was also found that, the cellulose-based polymers achieved an excellent solubility in organic solvents, such as benzene, methylbenzene, and pyridine, with the introduction of hydrophobic side chain into the cellulose backbone. Furthermore, it was found that these hydrophobic cellulose derivatives could self-assemble into spherical nanoparticles in aqueous solution, which indicates a tremendous potential of applications in pharmaceutical and medical fields.

Keywords Cellulose-based polymers · Acylation · Self-assembly

---

Y. Guo · X. Wang (✉) · D. Li · H. Du · X. Wang · R. Sun (✉)
State Key Laboratory of Pulp and Paper Engineering, South China University of Technology,
Guangzhou 510640, China
e-mail: fewangxh@scut.edu.cn

R. Sun
e-mail: ynsun@scut.edu.cn

R. Sun
Institute of Biomass Chemistry and Technology, Beijing Forestry University, Beijing 100083, China

Introduction

Cellulose, composed of β ($1 \rightarrow 4$) linked D-glucose units, is the most abundant polysaccharide polymer in the organic world [1]. It has been estimated that about 10^{12} tons of cellulose were generated by photosynthesis of plants every year throughout the world [2]. This inexpensive, limitless, and renewable resource has been widely studied during the past decades owing to its great potential of substituting fossil-based chemical products [3, 4]. Unfortunately, the poor solubility of cellulose in water and most organic solvents has limited its application.

After appropriate functionalization or chemical modification, cellulose can be tailored to have good solubility and desired properties. The typical examples include cationic cellulose [5, 6], acylated cellulose [7, 8], etherificated cellulose [9–12], hydrophobic cellulose [13–17] as well as amphiphilic cellulose [18–22]. Owing to their non-toxicity, biotolerability, biodegradability, and chemical stability, these cellulose-based polymers can be used as functional biomaterials, bioplastics, and bioenergy to reduce global dependence on the fossil resources.

Among these various cellulose-based polymers, the hydrophobic associating cellulose with long hydro-carbon chains has attracted growing attention since the pioneering work of Landoll [13], who firstly prepared the hydrophobic cellulose from water-soluble cellulose derivatives (such as hydroxyethyl cellulose, carboxymethyl cellulose, and methyl cellulose). Now there have appeared large quantities of literatures concerning of this kind of polymers [23–29]. After partial hydrophobization, the cellulose derivatives can be dissolved in common organic solvents, which makes the further functionalization much easier and better controlled. More importantly, the polymers consisting of both hydrophilic and hydrophobic segments can form micelle-like self-assemblies with hydrophobic core and hydrophilic shell in aqueous media via non-covalent intra- and/or intermolecular association of hydrophobic segments [30]. Such types of self-assemblies are good delivery vehicles for bioactive or functional agents of poor solubility. The solubility and the self-assembly behaviors of these hydrophobic associating cellulose derivatives generally correlate with their hydrophobic nature [20, 31, 32]. However, most hydrophobic associating cellulose-based polymers were prepared in heterogeneous system from water soluble cellulose derivatives, in which the degree of hydrophobic substitution is difficult to be controlled.

In this paper, the hydrophobic cellulose derivatives were prepared by the homogeneous acylation of cellulose with octanoyl, lauroyl, and palmitoyl chlorides in the solvent of DMAc/LiCl. The structures of these cellulose derivatives were clarified by elemental analysis, FT-IR, CP/MAS ^{13}C NMR, and their crystal structure and thermal properties were characterized by X-ray diffraction and thermogravimetry, respectively. A definite control over the hydrophobic nature of these derivatives was realized by varying the chain length of fatty acyl chlorides and the molar ratio of acyl chlorides vs anhydroglucose unit. The self-assembled nanoparticles of the cellulose derivatives with spherical geometry and controllable size in the range of around 50–100 nm were prepared in aqueous solution by a dialysis method.

Experimental

Reagent and materials

Microcrystalline cellulose (MCC) (Daojun Trading Company, Guangzhou, China) with particle size of 50 μm was firstly dried in vacuum for 1 h at 100 °C before use. All commercial chemicals were of reagent grade or better, in which octanoyl chloride, lauroyl chloride, palmitoyl chloride, methanol, dioxane, benzene, and ethanol were used without further purification, while dimethylacetamide (DMAc), dimethylaminopyridine (DMAP), lithium chloride (LiCl), and pyridine were dried and purified before use.

Homogeneous synthesis of hydrophobically modified cellulose

MCC (2 g) was fed into a three-necked flask provided with a condenser. Then, 50 ml DMAc (and DMAP for octanoyl chloride) was added and MCC was dispersed therein by stirring for 30 min at 160 °C to give slurry. After the slurry had been cool to 80 °C, 4.5 g dried LiCl was added. Then the mixture was stirred at this temperature for additional 3 h, before cooled down to room temperature and stirred for overnight. The transparent cellulose solution was obtained.

The above MCC solution was heated to 60 °C in an oil bath. Then equimolar fatty acyl chloride in 50 ml DMAc was added dropwise into it. In this case, pyridine (10 ml) was subsequently added under stirring in order to counteract the HCl generated during the esterification process. Then the homogeneous reaction mixture was stirred for additional 3 h at 60 °C. When the reaction was ended, the mixture was cooled down to room temperature and precipitated with methanol. Subsequently, the product was isolated by centrifugation, and then, purified by washing with methanol for several times. Finally, the product was vacuum dried at 50 °C for 12 h.

Solubility test

The solubilities of cellulose and its hydrophobic derivatives in dichloromethane, chloroform, benzene, methyl benzene, pyridine, tetrahydrofuran (THF), dioxane, dimethyl formamide (DMF), and dimethylsulfoxide (DMSO) were evaluated in this experiment. Ten milligram of each sample was placed in a test tube with 4 ml each of solvent. After mixing with a vortex mixer and followed by an ultrasonic treatment, the mixture was stored at room temperature for 5 days and observed visually [33].

Self-assembly of hydrophobically modified cellulose

At room temperature, hydrophobically modified cellulose (HPMC) was dissolved in 1 ml DMSO solvent and then 10 ml deionized water was added dropwise under vigorous stirring. The solution was dialysed (MWCO 3.0 kDa) against deionized water for 72 h to completely remove DMSO. The solution inside the dialysis bag was collected and diluted to a certain concentration with deionized water.

Characterization

The Fourier transform infrared (FT-IR) spectra of all hydrophobic-modified cellulose derivatives were recorded from KBr pellets containing 1 % finely ground samples on a spectrophotometer (Nicolet 750). The range of all spectra was from 4,000 to 400 cm^{-1}.

Solid-state cross polarization magic angle spinning carbon-13 nuclear magnetic resonance (CP/MAS ^{13}C NMR) spectra were recorded using a Bruker MSL 300 MHz spectrometer operating in the FT mode at room temperature (25 °C) and 74.5 MHz. About 100 mg of samples were packed into 4 mm zirconia rotors for MAS at approximately 4 kHz. The contact time and repetition time were 1 ms and 2 s, respectively.

Elemental analysis (C, H, O) was carried out by means of a VARIO EL III analyzer and the DS (degree of substitution) value of acyl chlorides groups was calculated according to the carbon content, as the following formula.

$$\mathrm{DS} = \frac{M_{\mathrm{AGU}} \times \mathrm{C}\,\% - 12 \times 6}{12 \times N - M \times \mathrm{C}\,\%}$$

where DS, M_{AGU}, C %, N, M delegated the degree of substitution of acyl chlorides, the molecular weight of anhydroglucose unit, the content of element carbon, the number of carbon in the acyl chlorides, and the molecular weight of acyl chlorides, respectively.

X-ray diffraction (XRD) was determined by a D8 ADVANCE X-ray diffractometer, in which the high-intensity monochromatic nickel-filtered CuKα radiation was generated at 40 kV and 40 mA. Samples were scanned at a speed of 1°/min, range from 2θ 5 to 40° with a step size of 0.04° at room temperature.

Thermal analysis of the cellulose-based hydrophobic samples was preformed using thermogravimetric analysis (TGA) and differential scanning calorimetry (DSC) on a simultaneous thermal analyzer (Pyris Diamond TG/DTA, PE Instrument). The apparatus was continually flushed with nitrogen. The samples were weighed between 8 and 12 mg. Each sample was heated from room temperature to 600 °C at a rate of 10 °C min^{-1}.

The transmission electron microscopy (TEM) images were observed on a JEM-100CXII instrument operating at an accelerator voltage of 120 kV.

The average hydrodynamic particle size of HPMC in aqueous media was determined by dynamic light scattering (DLS, Malvem 90 plus particle size analyzer) at the wavelength of 659 nm with a semiconductor laser diode (30 mW) as the light source. The scattering angle was fixed at 90° and the temperature was performed at 25 °C. The concentration of HPMC in deionized water was 0.1 mg/ml.

Results and discussion

Synthesis of hydrophobically modified cellulose

Owing to its high crystallinity and strong inter- and intra-molecular hydrogen bonds, natural cellulose has poor solubility in water, and common organic solvents. The

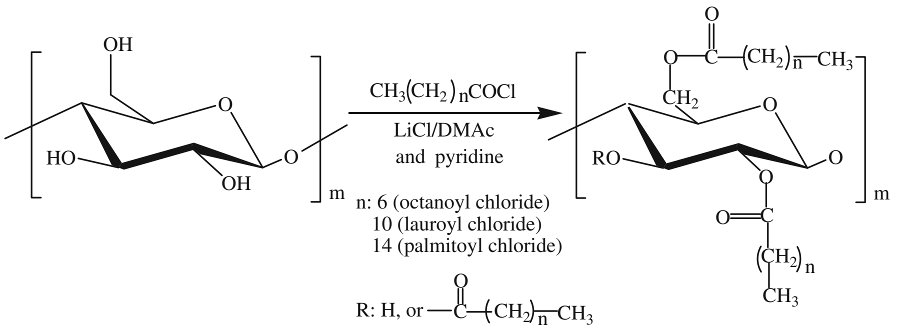

Fig. 1 Synthetic procedure of cellulose-based hydrophobically associating polymers

most versatile and widely applied solvents of cellulose are binary mixtures of polar organic liquids and inorganic salts, for example DMAc/LiCl. However, due to the strong hydrogen bonds and crystalline structure of cellulose, activating pretreatment must be carried out to make cellulose well dissolved in DMAc/LiCl solvent. Several pretreatment methods have been reported, including alkalization, acidic activation, continuous disturbing and high-temperature treatment, etc. [34–36]. After exploring the different activation methods, we found that stirring cellulose in DMAc at 160 °C for half an hour and adding anhydrate LiCl salt after the mixture was cooled to 80 °C could obtain very clear and homogenous cellulose solution. In this study, the cellulose was dissolved in DMAc/LiCl solvent and the acylation reactions were performed in the homogeneous system. Furthermore, pyridine was used as the acid scavenger.

The synthetic procedure was presented in Fig. 1. The hydrophobic cellulose derivatives with different aliphatic side chain length (with different carbon number of 8, 12, and 16) were defined as follows: cellulose octanoate (CO), cellulose lauroate (CL), cellulose palmitoate (CP).

The hydrophobically modified cellulose derivatives with varying degree of substitution (DS) were also prepared. According to the results of elemental analysis, the DS values of cellulose derivatives samples were ranged from 0.02 to 1.75 (Table 1). In general, the DS and yields of the products increased appreciably with increasing molar ratios of acyl chloride versus AGU, except octanoyl chloride, of which, the DS had reached a maximum value at the molar ratio of 3:1 and then followed by a small decrease for 4:1. This decrease could be explained by the fact that the acylation reaction between cellulose and acyl chlorides was a reversible reaction. With increasing the amount of acyl chlorides, the rate of acylation was increased. But when the DS was above 1.75, the steric resistance of molecular increased, which was less favorable for the proceeding of acylation reaction, meanwhile the reverse reaction of acylation such as partial hydrolysis of the ester groups was further enhanced [37]. At the same molar ratio, the DS of cellulose octanoate (C8) was much higher than that of cellulose lauroate (C12) and palmitoate (C16), because the reactivity of the fatty acyl chlorides was strongly affected by the chain length. Sealey et al. [38] had found the same phenomenon in the acylation reaction between cellulose and acetyl chlorides.

Table 1 Conditions and results of the cellulose-based hydrophobic polymers

No.	Reactants	Amount[a] (molar ratio)	Yield (%)	Elemental analysis (%)			DS[b]
				C	H	O	
CP1	Palmitoyl chloride	2:1	35.8	49.7	7.4	42.9	0.12
CP2	Palmitoyl chloride	3:1	64.3	54.9	8.9	36.2	0.28
CP3	Palmitoyl chloride	4:1	76.2	58.6	7.4	34.2	0.44
CL1	Lauroyl chloride	2:1	15.3	45.2	7.7	47.1	0.02
CL2	Lauroyl chloride	3:1	17.2	49.1	7.5	43.5	0.13
CL3	Lauroyl chloride	4:1	12.4	45.2	7.6	39.8	0.33
CO1	Octanoyl chloride	2:1	15.3	51.7	8.6	39.6	0.39
CO2	Octanoyl chloride	3:1	17.2	62.5	10.0	27.6	1.75
CO3	Octanoyl chloride	4:1	12.4	61.5	9.7	28.8	1.55

[a] Mol ratio of acyl chloride vs anhydroglucose unit (AGU)

[b] Degree of substitution was estimated by elemental analysis

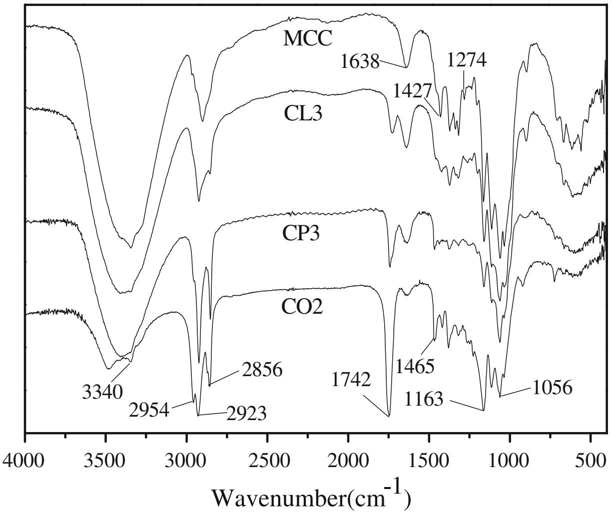

Fig. 2 FT-IR spectra of cellulose, CO2, CP3, and CL3

FT-IR spectroscopy

The FT-IR spectra of MCC and its acylated derivatives with different chain length are shown in Fig. 2. Compared with that of MCC, the intensity of the wide peak at 3,340 cm^{-1} corresponding to the stretching vibration of –OH group decreased in the spectra of cellulose derivatives, which indicates acylation occurred at the hydroxyl sites of MCC. The absorption bands at 2954, 2856 cm^{-1}, and that at 1,465 cm^{-1} assigned to C–H stretching and C–H bending, respectively, become stronger and sharper in the spectra of cellulose derivatives. It suggests that alkyl groups have

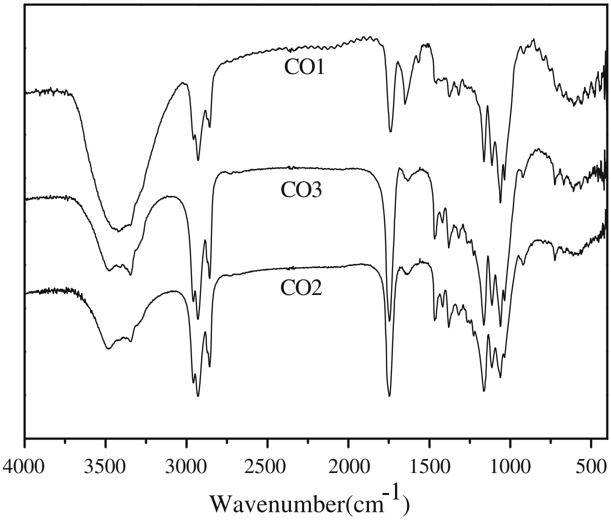

Fig. 3 FT-IR spectra of CO with different DS

been successfully introduced into the backbone of cellulose moieties. Comparing the FT-IR spectra of cellulose derivatives with unmodified cellulose, it could be clearly observed that a new ester carbonyl band at 1,742 cm^{-1} appeared, which confirmed a successful acyl substitution. Moreover, the absence of absorbance at 1,570 cm^{-1} corresponding to the antisymmetric stretching of carboxylic anions [39] in the spectra of cellulose esters indicates that the products are free of the hydrolyzate of fatty acyl chloride.

The mol ratio of acetyl chloride versus anhydroglucose unit is a key parameter affecting the acylation of cellulose. As an example, the FT-IR spectra of the cellulose octanoate derivatives (C8) obtained with different mol ratios of acetyl chloride versus AGU are shown in Fig. 3. It can be found that their FT-IR spectra exhibit a similar trend with that of DS determined by elemental analysis. As the value of DS is increased from 0.39 (spectrum CO1) to 1.75 (spectrum CO2), the peak at 1,742 cm^{-1} corresponding to ester carbonyl band and the peaks at 2954, 2856, and 1465 cm^{-1} assigned to C–H bands increase accordingly. On the other hand, the intensity of wide peak of –OH group at 3,340 cm^{-1} decreased with the increasing of DS values.

In addition, the FT-IR analysis also indicates the enhancement of the hydrophobic nature of cellulose derivatives, because the band at 1,638 cm^{-1} corresponding to the bending mode of the absorbed water molecules [26] is weakened after acylation (Fig. 2), and its intensity reduces significantly with the increasing of DS values (Fig. 3).

Solid-state CP/MAS ^{13}C NMR

Figure 4 shows the solid-state CP/MAS ^{13}C NMR spectra of MCC (a) and CO2 (b). In Fig. 4a, the signals shown at 105.62 (C-1), 105.03 (C-1), 103.99 (C-1), 88.76 (C-4),

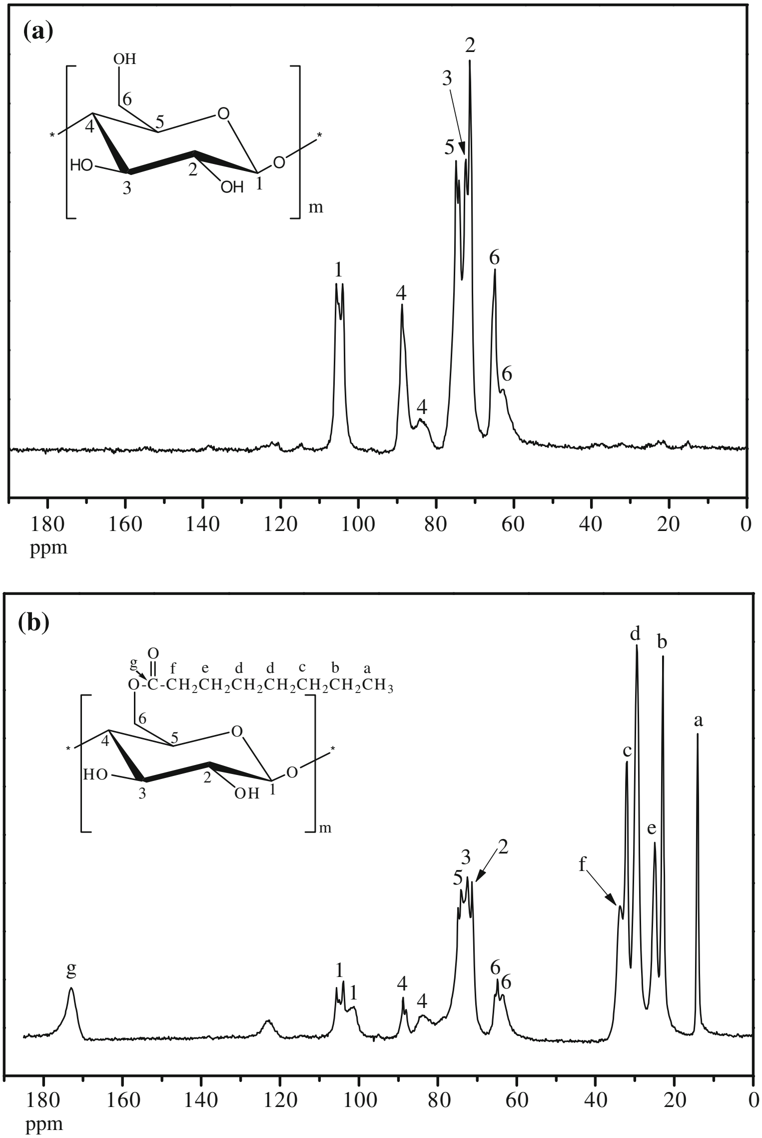

Fig. 4 CP/MAS ^{13}C NMR spectra of MCC (**a**) and CO2 (**b**)

84.12 (C-4), 74.81 (C-5), 74.06 (C-5), 72.37 (C-3), 71.26 (C-2), 64.87 (C-6), and 62.89 (C-6) are attributed to the carbons in the anhydroglucose unit structure. In the CP/MAS ^{13}C NMR spectrum of CO2 (Fig. 4b), the signals of the carbon atoms of modified anhydroglucose unit are detectable in the region of 105.62–63.55 ppm. The peaks assigned to C-4 and C-6 in crystalline (at 88.76, 64.87 ppm) and disordered cellulose (at 84.12, 62.89 ppm) could also be identified in the spectra [40]. In comparison with those of the raw materials, the increased signal of the disordered cellulose peaks and the reduced signal of crystalline cellulose peaks demonstrate that the crystalline structure has been partially destroyed in the derivatives.

It is worthy to note that a new single peak at 101.23 ppm appears in the spectrum of CO2, which is attributed to C-1 of the polysaccharide structure. The signals of the incorporated aliphatic carbon atoms appear at high magnetic fields, and are sufficiently separated from those of the saccharidic moieties. The chemical shifts at 14.06 and 172.6 ppm are assigned to the methyl carbon atoms and carbonyl carbon of octanoyl groups, respectively. The single resonance of the methylene carbon at the position b of the octanoyl groups is shown at 22.86 ppm, while the signals of internal methylene carbons at the positions of e, d, c, f, appeared at 24.90, 29.44, 32.02, and 33.75 ppm, respectively [41]. These evidences obviously support the successful occurrence of acylation between cellulose and acyl chlorides in DMAc/LiCl and the introduction of alkyl groups into the moiety of cellulose.

X-ray diffraction

The crystalline character of cellulose that resulted from the great intra- and intermolecular hydrogen bonds distinguishes it from the most carbohydrate polymers. As shown in Fig. 5, the microcrystalline cellulose displays the typical XRD pattern of cellulose I, with the main diffraction peaks at around 2θ 14.95°, 16.54°, 22.66°, and 34.60°, normally corresponding to the diffraction planes 101, 10$\bar{1}$, 002, and 040, respectively. In the XRD spectra of cellulose derivatives, the characteristic peaks of 101, 002, and 040 planes have been weakened or disappeared, while a new broad diffraction peak between $2\theta = 18°$ and 21° is obviously observed, which is normally attributed to the amorphous regions of cellulose chains [42]. Similar results had been reported by Freire et al. [26]. The weakening and lose of diffraction

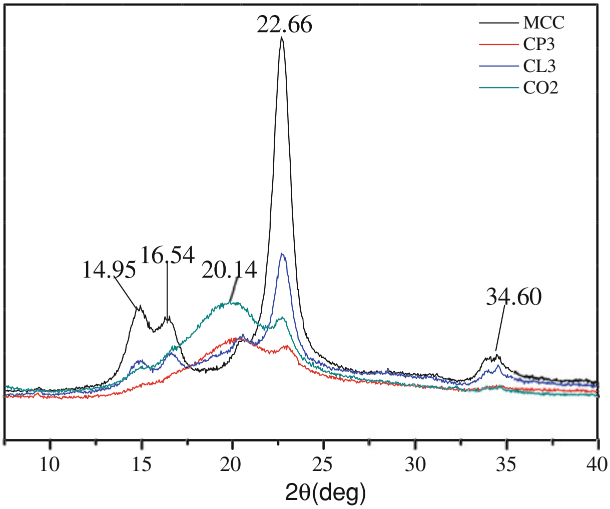

Fig. 5 XRD spectra of MCC, CO, CL, and CP

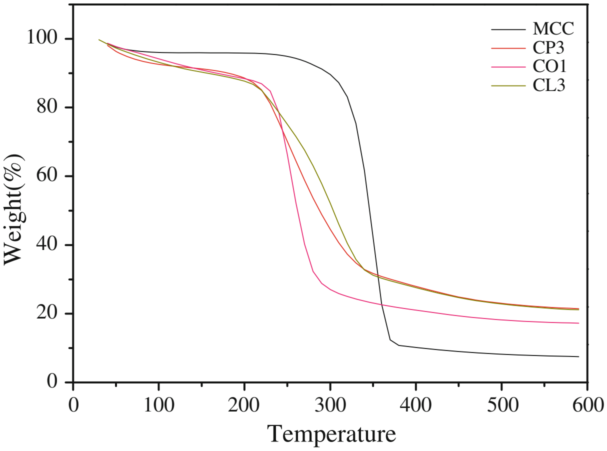

Fig. 6 TG curves of MCC, CO, CL, and CP

peaks of cellulose I after acylation may be explained by the loss of hydrogen bonds, as discussed previously in the FT-IR and CP/MAS ^{13}C NMR analysis.

Thermal analysis

It is reported that the substituent groups have an important influence in the thermal stability of cellulose and its derivatives [43–45]. Therefore, the thermal behaviors of microcrystalline cellulose and its hydrophobic derivatives with different chain length and similar DS were characterized. Their thermogravimety (TG) curves are shown in Fig. 6, and the analysis results are listed in Table 2. According to Fig. 6, after initial small weight loss of moisture at 100–120 °C, the decomposition begins at about 271, 215, 216, and 209 °C for cellulose, cellulose octanoate, cellulose laureate, and cellulose palmitate, respectively. Then a major decomposition temperature (T_{dm}, the temperature at the maximum rate of weight loss) proceeds at 351, 248, 301, and 261 °C for cellulose and its derivatives, respectively. The loss of weight at the major decomposition temperature for those samples was 58, 34, 48, and 36 %, respectively. From the figures, it could be clearly found that the initial decomposition temperature (T_{di}), the final decomposition temperature (T_{df}), and the temperature at the maximum rate of weight loss (T_{dm}) of hydrophobic celluloses are all lower than those of the cellulose. These results suggest a reduced thermal

Table 2 The thermal stabilities of cellulose and its hydrophobic derivatives

Samples	T_{di} (°C)	T_{df} (°C)	T_{dm} (°C)	DS
MCC	271	379	351	–
CO1	215	305	248	0.39
CL3	216	350	301	0.33
CP3	209	343	261	0.44

stability of cellulose derivatives, which is possibly caused by the introduction of less stable side chains. Moreover, since the crystalline structure of cellulose has been greatly destroyed after the acylation reaction, the derivatives with looser and disordered crystalline structure are more easily decomposed by thermal treatment.

Solubility of hydrophobically modified cellulose

The solubility of cellulose derivatives depends on the nature of the substituent, the degree of substitution, and the distribution of substituted sites. To investigate the solubility of the hydrophobic cellulose derivatives, many kinds of solvents were applied in this study and the solubility test results are given in Table 3. After the hydroxyl groups of cellulose were partly substituted by acyl groups, they showed an excellent solubility in a variety of organic solvents, such as benzene, methylbenzene and pyridine, and yielded transparent solutions. However, they were insoluble in halogenated hydrocarbons, THF, and dioxane solvents. Compared with CL and CP, CO showed a better solubility in some polar solvents, like DMF, probably due to the enhanced DS. The improved solubility of cellulose derivatives in common organic solvents can be explained by the fact that the inter- and intra-molecular hydrogen bonds in the cellulose derivatives were weakened with the loss of –OH groups and the molecular structure became more expanded and disorganized as compared with microcrystalline cellulose.

Self-assembly of hydrophobically modified cellulose

Owing to the improved solubility of cellulose derivatives in organic solvents, the self-assembly of the polymers in aqueous solution was realized by a dialyzing method, in which the hydrophobic cellulose derivatives were firstly dissolved in a small volume of DMSO, then the self-assembly process was initiated by adding water drop-wise with stirring and accomplished by dialysis in water.

After dispersed in water, the cellulose derivatives had self-assembled micelle-like structure to minimize the surface-free energy, probably with a hydrophobic core and a hydrophilic shell, formed by hydrophobic interaction between hydrophobic side chains.

DLS is a common method to characterize the size and size distribution of particles in water. Figure 7 shows the DLS results for aqueous dispersion of hydrophobic cellulose derivatives particles with different chain length at similar DS.

Table 3 The solubilities of cellulose and the hydrophobic cellulose derivatives

	$CHCl_3$	CH_2Cl_2	C_6H_6	$C_6H_5CH_3$	Pyridine	THF	Dioxane	DMF	DMSO
MCC	×	×	×	×	×	×	×	×	×
CP3	×	×	○	○	○	×	×	△	△
CL3	×	×	○	○	○	×	×	△	△
CO2	△	△	○	○	○	×	×	○	○

Triangle swelling, *circle* dissolved, *times* not dissolve

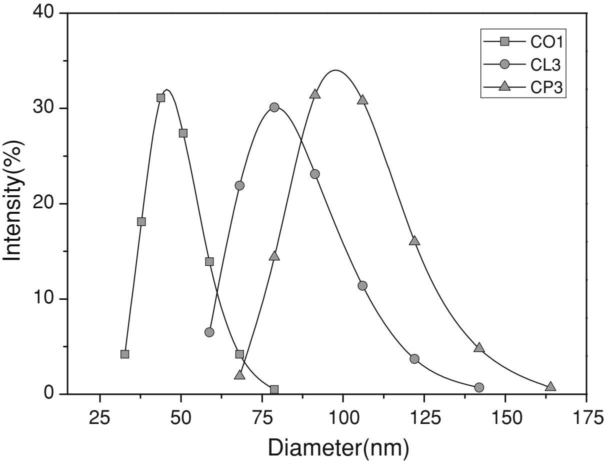

Fig. 7 DLS results of CO, CL, and CP self-assembled nanoparticles in water

It shows that the average hydrodynamic diameters (D_h) of the particles are 47.2, 81.1, and 101.4 nm for CO1, CL3, and CP3, respectively. The peak width represents the size distribution of the particles. It is notable that CO1 has narrower size distribution than CL3 and CP3. The difference in the size and size distribution is probably caused by the different graft chain length and M_w of the samples. The derivatives with shorter side chains have smaller M_w and tend to self-assemble into smaller particles with narrower size distribution.

TEM measurement was conducted to observe the morphology and size of the particles directly. TEM image of CO1 particle in water (Fig. 8) reveals that the hydrophobic cellulose derivatives self-assemble into well-defined spherical nanoparticles. According to the TEM results, most CO1 particles in water have diameters of around 50 nm, which is consistent with the results of DLS. It is noticed that there

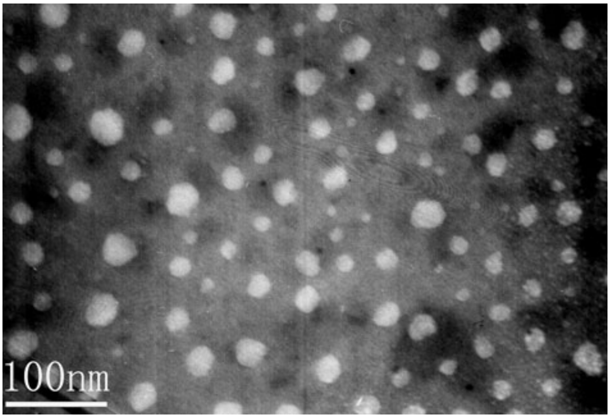

Fig. 8 TEM image of CO self-assembled nanoparticles

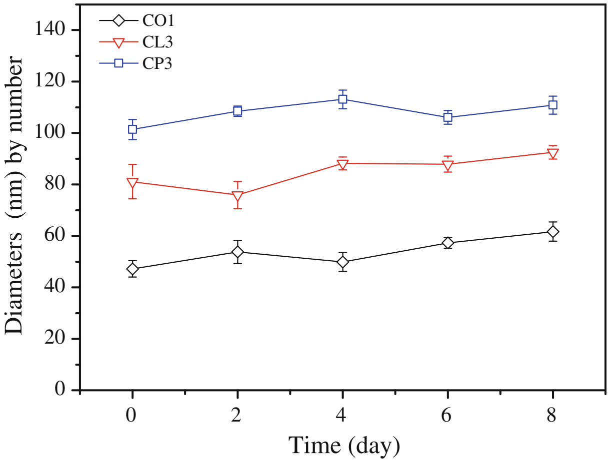

Fig. 9 The diameter of nanoparticles from CO1, CL3, and CP3 in pure water at room temperature as a function of time

are also some small particles with size of around 20–30 nm shown in the picture, which may have resulted from the diversity in the chain length of cellulose raw materials.

The stability of the self-assembled nanoparticles is very important for their clinical application as drug delivery carriers. And it is more desirable to get stable and nano-sized particles from cellulose derivatives, because the insolubility of cellulose in aqueous solution often led to aggregation and precipitation of particles within a few days. The stability of HPMC self-assembled particles was investigated by measuring the mean diameter of particles from CO1, CL3, and CP3 samples in aqueous solution as the storing time prolonged (Fig. 9). It can be seen that the diameters of all the three nanoparticles are kept constant when stored at room temperature for almost 8 days, suggesting that they are very stable.

Conclusion

From the results it can be concluded that the homogeneous acylation of cellulose with octanoyl, lauroyl, and palmitoyl chlorides was realized in DMAc/LiCl solvent by using pyridine as acid scavenger. Taking advantage of the homogeneous reaction, the acylation degree could be easily controlled in a wide range (from 0.02 to 1.75). After modification, the crystalline degree and the thermal stability of cellulose derivatives were reduced, while the hydrophobic character of cellulose was improved. These cellulose derivatives achieved improved solubility in common organic solvents, and can self-assemble into spherical nanoparticles in aqueous solution. Potential applications of these hydrophobic cellulose derivatives and their self-assembled nanoparticles in wider field could be expected.

Acknowledgments This study was supported by the grants from National Science Foundation of China (No. 51103046); Ministry of Science and Technology, 973 project (No. 2010CB732204); Fundamental Research Funds for the Central Universities, SCUT; and Key Laboratory of Renewable Energy and Gas Hydrate, Chinese Academy of Science (No. 0907k4).

References

1. Kim J, Yun S (2006) Discovery of cellulose as a smart material. Macromolecules 39(12):4202–4206
2. Hon DNS, Yan H (2001) Cellulose furoate. I. synthesis of homogeneous and heterogeneous systems. J Appl Polym Sci 81(11):2649–2655
3. Edgar KJ, Buchanan CM, Debenham JS, Rundquist PA, Seiler BD, Shelton MC, Tindall D (2001) Advances in cellulose ester performance and application. Prog Polym Sci 26(9):1605–1688
4. Klemm D, Schumann D, Kramer F, Heßler N, Koth D, Sultanova B (2009) Nanocellulose materials-different cellulose, different functionality. Macromol Symp 280(1):60–71
5. Tan SB, Zhang LM, Li ZM (1998) Synthesis and characterization of new amphoteric graft copolymer of sodium carboxymethyl cellulose with acrylamide and dimethylaminoethyl methylacrylate. J Appl Polym Sci 69(5):879–885
6. Koschella A, Heinze T (2001) Novel regioselectively 6-functionalized cationic cellulose polyelectrolytes prepared via cellulose sulfonates. Macromol Biosci 1(5):178–184
7. Marson GA, El Seoud OA (1999) A novel, efficient procedure for acylation of cellulose under homogeneous solution conditions. J Appl Polym Sci 74(6):1355–1360
8. Barthel S, Heinze T (2006) Acylation and carbanilation of cellulose in ionic liquids. Green Chem 8(3):301–306
9. Blasutto M, Delben F, Milost R, Painter TJ (1995) Novel cellulosic ethers with low degrees of substitution-I. Preparation and analysis of long-chain alkyl ethers. Carbohydr Polym 27(1):53–62
10. Vaca-Garcia C, Thiebaud S, Borredon ME, Gozzelino G (1998) Cellulose esterification with fatty acids and acetic anhydride in lithium chlorides/*N,N*-dimethylacetamide medium. J Am Oil Chem Soc 75(2):315–319
11. Torri G, Cosentino C, Delben F, Simonutti R, Sozzani P (1999) Novel cellulosic ethers with low degrees of substitution-II. Magic angle spinning NMR study. Carbohydr Polym 40(2):125–135
12. Yue ZL, Cowie JMG (2002) Preparation and chiroptical properties of a regioselectively substituted cellulose ether with PEO side chains. Macromolecules 35(17):6572–6577
13. Landoll LM (1982) Nonionic polymer surfactants. J Polym Sci A 20(2):443–455
14. Heinze T (1998) New ionic polymers by cellulose functionalization. Macromol Chem Phys 199(11):2341–2364
15. Charpentier-Valenza D, Merle L, Mocanu G, Picton L, Muller G (2005) Rheological properties of hydrophobically modified carboxymethylcellulose. Carbohydr Polym 60(1):87–94
16. Wang CQ, Tan HM, Dong YP, Shao ZQ (2006) Trimethylsilyl hydroxypropyl cellulose: preparation, properties and as precursors to graft copolymerization of ε-caprolactone. React Funct Polym 66(10):1165–1173
17. Wei YP, Cheng F (2007) Synthesis and aggregates of cellulose-based hydrophobically associating polymer. Carbohydr Polym 68(4):734–739
18. Nishimura H, Donkai N, Miyamoto T (1997) Preparation and properties of a new type of comb-shaped, amphiphilic cellulose derivative. Cellulose 4(2):89–98
19. Danilevicius A, Dobiliene J, Wutz C, Liesiene J (2007) Phenoxyhydroxypropylhydroxyethylcellulose-new amphiphilic cellulose derivative. Cellulose 14(4):321–329
20. Wei YP, Cheng F, Hou GL, Sun SF (2008) Amphiphilic cellulose: surface activity and aqueous self-assembly into nano-sized polymeric micelles. React Funct Polym 68(5):981–989
21. Yang LQ, Kuang JL, Li ZQ, Zhang BF, Cai X, Zhang LM (2008) Amphiphilic cholesteryl-bearing carboxymethylcellulose derivatives: self-assembly and rheological behavior in aqueous solution. Cellulose 15(5):659–669
22. Shi RW, Burt HM (2002) Synthesis and characterization of amphiphilic hydroxypropylcellulose-graft-poly(ε-caprolcatone). J Appl Polym Sci 89(3):718–727
23. Li Q, Ye L, Cai Y, Huang RH (2006) Study of rheological behavior of hydrophobically modified hydroxyethyl cellulose. J Appl Polym Sci 100(4):3346–3352

24. Ye L, Li Q, Huang RH (2006) Study on the rheological behavior of the hydrophobically modified hydroxyethyl cellulose with 1,2-epoxyhexadecane. J Appl Polym Sci 101(5):2953–2959
25. Dai SS, Ye L, Huang RH (2006) A study on the solution behavior of IPBC-hydrophobically-modified hydroxyethyl cellulose. J Appl Polym Sci 100(4):2824–2831
26. Freire CSR, Silvestre AJD, Pascoal Neto C, Belgacem MN, Gandini A (2006) Controlled heterogeneous modification of cellulose fibers with fatty acids: effect of reaction conditions on the extent of esterification and fiber properties. J Appl Polym Sci 100(2):1093–1102
27. Chen R, Yi CB, Wu H, Guo SY (2009) Solid state mechano-chemical grafting copolymerization of hydroxyethyl cellulose with acrylic acid. J Appl Polym Sci 112(6):3537–3542
28. Cunha AG, Gandini A (2010) Turning polysaccharides into hydrophobic materials: a critical review. Part 1. Cellulose 17(5):875–889
29. Jiang C, Wang XL, Sun PD, Yang C (2011) Synthesis and solution behavior of poly(ε-caprolactone) grafted hydroxyethyl cellulose copolymers. Int J Biol Macromol 48(1):210–214
30. Photos PJ, Bacakova L, Discher B, Bates FS, Discher DE (2003) Polymer vesicles in vivo: correlations with PEG molecular weight. J Controlled Release 90(3):323–334
31. Huang YP, Yu HL, Guo L, Huang QR (2010) Structure and self-assembly properties of a new chitosan-based amphiphile. J Phys Chem B 114(23):7719–7726
32. Liu KH, Chen BR, Chen SY, Liu DM (2009) Self-assembly behavior and doxorubicin-loading capacity of acylated carboxymethyl chitosans. J Phys Chem B 113(35):11800–11807
33. Jiang GB, Quan DP, Liao HP, Wang HH (2006) Preparation of polymeric micelles based on chitosan bearing a small amount of highly hydrophobic groups. Carbohydr Polym 66(4):514–520
34. Chauvelon G, Saulnier L, Buleon A, Thibault J-F, Gourson C, Benhaddou R, Granet R, Krausz P (1999) Acidic activation of cellulose and its esterification by long-chain fatty acid. J Appl Polym Sci 74(8):1933–1940
35. Wang PL, Tao BY (1994) Synthesis and characterization of long-chain fatty acid cellulose ester (FACE). J Appl Polym Sci 52(6):755–761
36. Röder T, Morgenstern B (1999) The influence of activation on the solution state of cellulose dissolved in *N*-methylmorpholine-*N*-oxide-monhydrate. Polymer 40(14):4143–4147
37. Song Q, Yang YQ (2011) Preparation of cellulose laurate and characterization of its structure and performance. J Nanjing Univ (Natural Science Edition) 35(4):92–95
38. Sealey JE, Samaranayake G, Todd JG, Glasser WG (1996) Novel cellulose derivatives. IV. Preparation and thermal analysis of waxy esters of cellulose. J Polym Sci 34(9):1613–1620
39. Liu CF, Sun RC, Zhang AP, Ren JL (2006) Preparation of sugarcane bagasse cellulosic phthalate using an ionic liquid as reaction medium. Carbohydr Polym 68(1):17–25
40. Sun XF, Sun RC, Tomkinson J, Baird MS (2004) Degradation of wheat straw lignin and hemicellulosic polymers by a totally chlorine-free method. Polym Degrad Stab 83(1):47–57
41. Ilayaraja N, Manivel A, Velayutham D, Noel M (2008) Effect of alkyl chain length on the electrochemical perfluorination of n-alkane (C6–C10) carboxylic acid chlorides. J Appl Electrochem 38(2):175–186
42. Jandura P, Kokta BV, Riedl B (2000) Fibrous long-chain organic acid cellulose esters and their characterization by diffuse reflectance FTIR spectroscopy solid-state CP/MAS ^{13}C NMR, and X-ray diffraction. J Appl Polym Sci 78(7):1354–1365
43. Nada AMA, Hassan ML (2000) Thermal behavior of cellulose and some cellulose derivatives. Polym Degrad Stab 67(1):111–115
44. Heinze T, Schaller J (2000) New water soluble cellulose esters synthesized by an effective acylation procedure. Macromol Chem Phys 201(12):1214–1218
45. Heinze T, Liebert TF, Pfeiffer KS, Hussain MA (2003) Unconventional cellulose esters: synthesis, characterization and structure-property relations. Cellulose 10(3):283–296